ELSEVIER

Journal of Alloys and Compounds 218 (1995) 17–21

Journal of ALLOYS AND COMPOUNDS

Characterization of the Nd–Fe–Al μ phase in the microstructure of an aluminium- and vanadium-substituted Nd–Fe–B magnet

L. Legras, J. Delamare, D. Lemarchand, J. Vu Dinh, P. Vigier

Laboratoire de Microscopie Electronique et Matériaux Magnétiques, Groupe de Métallurgie Physique URA CNRS 808, Université de Rouen, 76821 Mont-Saint-Aignan Cedex, France

Received 31 May, 1994

Abstract

The microstructure of a commercial Nd–Fe–B-based magnet containing aluminium and vanadium is investigated by transmission electron microscopy. Two kinds of μ (Nd–Fe–Al) precipitates are identified: thin platelets along Φ-phase grain boundaries, and thicker lamellae inside the triple junction Nd-rich phase. The morphology of the μ phase and its solidification mechanism are shown to be similar in the magnet and in ternary Nd–Fe–Al alloys. However, a structural modification of the μ phase takes place in the magnet in comparison with the ternary alloys.

Keywords: Electron microscopy; Microstructure; Magnets; Polytypes

1. Introduction

Numerous addition elements are added to Nd–Fe–B permanent magnets to improve their magnetic and physical properties, or to favour the metallurgical process during their manufacture. These additives either dissolve in existing phases or stabilize new compounds in the magnet. Thus, the enhancement of magnets' properties results from both phase composition and microstructural modifications.

Al, for instance, is widely used as an additive to increase the coercivity of Nd–Fe–B-based permanent magnets. Al is partly dissolved in the Nd-rich phase of the magnet and enhances its liquid state wettability during the sintering heat treatment. The rest of the Al leads to the formation of two ternary compounds, i.e. δ phase ($Nd_{30}Fe_{70-x}Al_x$; $7<x<25$) and μ phase ($Nd_{33}Fe_{67-x}Al_x$; $2.5<x<5$), which are stable in the Al-poor part of the Nd–Fe–Al system [1,2]. Our paper aims to determine the microstructure of such an Al-doped magnet, using transmission electron microscopy. We focus our investigation on the formation and structure of the μ-phase, which has been identified as a secondary phase in this magnet.

The great number of additives in usual commercial magnets, and the interplay between these elements, make it difficult to analyze the individual effects of the additives. In this study, a better understanding of the role of Al is obtained by comparing the microstructure of the magnet with two Nd–Fe–Al model system alloys.

2. Experimental details

The microstructure of three specimens (S1, S2 and M) is examined and compared by transmission electron microscopy (TEM) and electron diffraction, using a 200 kV Jeol 2000 FX II model equipped with a Link energy-dispersive X-ray (EDX) analyser.

The compositions of the specimens are given in Table 1. Samples S1 and S2 are both ternary Nd–Fe–Al alloys. The composition of sample S1 is very close to that of the μ phase. This specimen was annealed at 500 °C for 30 days. Sample S2 is an as-cast Fe–Nd hypoeutectic alloy with a low Al content, simulating the behaviour of the Al-containing Nd-rich phase of the magnet.

Table 1
Composition of the samples studies (at.%)

	Nd	Dy	De	Co	Al	V	B
Sample S1	38		58.5		3.5		
Sample S2	67.8		30.9		1.3		
Sample M	13.5	1.5	67	5	1	4	8

SSDI 0925-8388(94)01369-1

Sample M is a commercial sintered UGISTAB 215-XH permanent magnet from AIMANTS UGIMAG.

The TEM samples were prepared by mechanical grinding, followed by a combination of electropolishing and Ar ion milling at 5 keV.

3. Results

3.1. Investigation of the Nd–Fe–Al alloys (samples S1 and S2)

The microstructure of the ternary Fe–Nd–Al alloy S1 is shown in Fig. 1. The constitution of this alloy is in agreement with the Nd–Fe–Al phase diagram and its liquidus projection as proposed by Grieb [2]. The solidification of sample S1 starts with the primary crystallization of the compound Nd_2Fe_{17} (bright areas in Fig. 1). Then, a peritectic reaction takes place between Nd_2Fe_{17} and the melt, which leads to the formation of the matrix μ phase (grey areas) around the Nd_2Fe_{17} crystals. Sample S1 mainly consists of the μ phase, which agrees with its composition (Table1).

Fig. 2 shows the microstructure of alloy S2. It is constituted of Nd_2Fe_{17} crystals formed during the primary solidification. They are distributed into two irregular lamellar eutectics: the first eutectic corresponds to the Nd_2Fe_{17}+Nd eutectic, whereas the second eutectic takes place at a smaller scale (typically 0.1 μm against 1 μm), and corresponds to the μ+Nd eutectic.

The case of the μ+Nd eutectic is illustrated by the TEM image in Fig. 3, which shows the detailed lamellar morphology of the μ-phase crystals embedded within the Nd phase. The crystals are clearly faceted (as discussed below) and often exhibit branching. Such branching commonly occurs during the growth of faceted eutectics. It originates from an instability of the front solidification, induced by competition between the capillarity and the diffusion process [3].

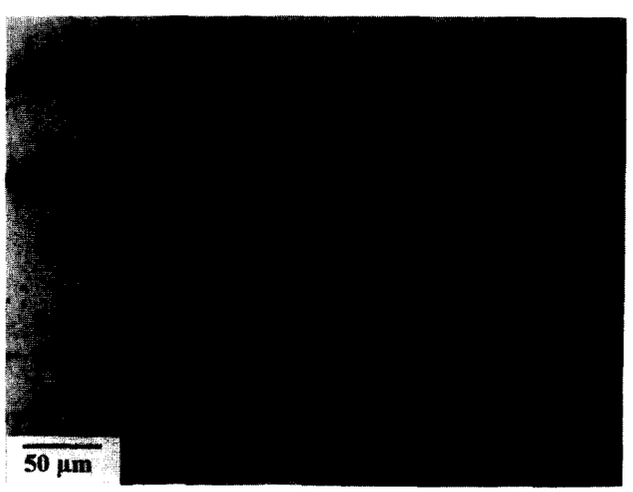

Fig. 1. Microstructure of sample S1, showing Nd_2Fe_{17} crystals (bright contrast) surrounded by μ phase (grey) and Nd (dark).

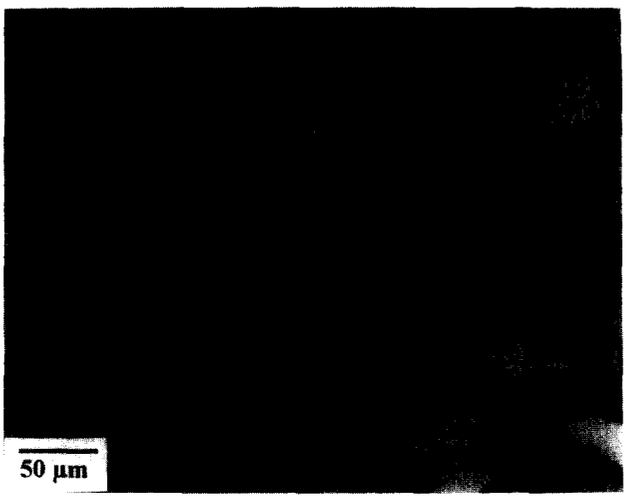

Fig. 2. Microstructure of sample S2, showing Nd_2Fe_{17} crystals within (Nd_2Fe_{17}+Nd) and (μ+Nd) lamellar eutectics.

Fig. 3. TEM image of sample S2, showing branched lamellar μ phase within Nd.

A previously published TEM study [4] has clarified the crystallography of the μ phase in these alloys. This compound is polytypic, i.e. its structure consists of a long-period stacking of identical layers. Each layer is constituted of a hexagonal array of structural units with parameters $a = 1.65$ nm (edge of the hexagon) and $c_0 = 1.20$ nm (height of each layer). The different layers are shifted by a translation vector parallel to their own plane, with respect to the previous layer in the stacking sequence.

Different crystal structure symmetries – either hexagonal (H) or rhombohedral (R) – result from the different possible stacking sequences of n layers. The corresponding crystal parameters are a and nc_0. Using Ramsdell notation for polytypes [5], these stacking variants are labelled nH or nR respectively. In Nd–Fe–Al alloys, different stacking sequences of the μ phase, such as 4H, 8H and 12R, have been recognized by TEM [6].

3.2. Investigation of the magnet (sample M)

3.2.1. Microstructure and characterization of the Al-free phases in the magnet

Fig. 4 shows a backscattered scanning electron microscopy (SEM) image of the sintered UGISTAB 215-XH magnet. The main features of the microstructure of this magnet have already been studied [7,8]. The matrix is constituted of the $Nd_2Fe_{14}B$ hard magnetic grains (Φ phase with grey contrast), and is surrounded by an Nd-rich phase, also present at triple junctions (bright contrast). EDX chemical analysis indicates that the Φ phase dissolves some Co, but no Dy was found (Table 2).

The addition of V in these magnets leads to improvements in the coercivity and corrosion resistance, which are associated with the formation of an intergranular $V_{3-x}Fe_xB_2$ boride ($x \approx 1$) [9,10]. This boride (and pores) shows up as the dark contrast in Fig. 4. This compound solidifies instead of the useless $Nd_{1.1}Fe_4B_4$ which exists in Nd–Fe–B-based magnets without V. The $V_{3-x}Fe_xB_2$ boride is generally several micrometres large and contains numerous crystallographic defects. Some spherical Nd-rich areas were found inside this boride. This is attributed to the complete immiscibility of Nd and V (as indicated by the binary Nd–V phase diagram), which induces segregation of these elements.

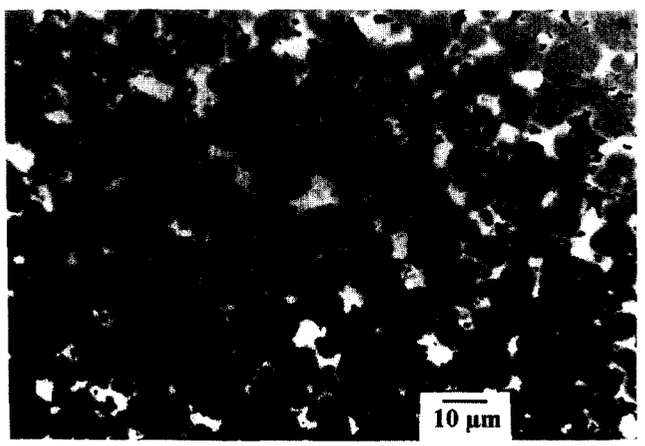

Fig. 4. Microstructure of sample M, showing Φ phase (grey contrast), Nd-rich phase (bright), $V_{3-x}Fe_xB_2$ boride and pores (dark).

Table 2
Mean atomic composition (at.%) of phases identified in the magnet (boron and oxygen not measured)

Phase	Nd	Dy	Fe	Co	Al	V
Φ phase	10		85	5		
$V_{3-x}Fe_xB_2$ (inter- and intragranular)			38	1		61
Spherical Nd-rich inclusion within intergranular $V_{3-x}Fe_xB_2$	39–49		34–48	11–16		1.5
FeV (σ phase) within Φ phase			48	2		50
Phase associated with σ within Φ phase	44	2	41	12		1
Spherical Nd-rich inclusion within Φ phase	81	4	13	2		

TEM studies show that the $V_{3-x}Fe_xB_2$ compound is also present within the hard magnetic Φ-phase grains, in the form of coherent precipitates with a typical size of several tens to several hundred nanometres. Their distribution is very inhomogeneous: some Φ-phase grains exhibit a high density of these precipitates, whereas others are free of them.

Moreover, TEM reveals several other minor phases inside the matrix of the magnet. Their composition is given in Table 2. A second kind of V-rich compound, with a Fe:V atomic ratio of almost 1:1, was identified as the σ phase of the Fe–V binary system. These precipitates are smaller than 50 nm and are embedded in an Nd–Fe–Co phase. Nd-rich spherical inclusions with a face centred cubic structure ($a = 0.52$ nm) are often detected within the Φ phase. The size of these inclusions is several hundred nanometres. Some of them were found with a fine precipitation of a V-containing phase, but its size (about 5 nm) prevented us from determining its structure and its composition.

3.2.2. Formation and characterization of the Al-stabilized μ phase in the magnet

In the Al-doped sintered magnet, no significant Al content was detected within the matrix Φ phase. This suggests the formation of an Al-stabilized compound, which is in agreement with previous studies [11,12]. Our TEM investigation effectively revealed the formation of the μ phase as an intergranular phase in the UGISTAB 215 XH magnet; in contrast, no evidence of the δ phase was found. This is probably because of the low Al content of the magnet (Table 1).

The μ-phase compound was mainly detected inside the Nd-rich triple junction phase, with a platelet shape (Fig. 5). The size of these platelets was several micrometres long and about 50 nm across. A typical electron diffraction pattern of the μ phase is shown in Fig. 6. It corresponds to the 2H stacking sequence, which is the simplest variant of the polytypic series. The lattice spacing of the μ phase in the TEM image is $d = 2c_0$, i.e. the spacing of (001) lattice planes of the 2H type. Depending on the defocus, some parts of the platelet image exhibit the split-periodicity c_0.

Our attempts to identify other kinds of stacking sequences of the μ phase in the magnet were unsuccessful; whereas different sequences were encountered in the ternary Nd–Fe–Al alloys [6], only the 2H variant has been observed in the magnet. This result means

Fig. 5. Microstructure of sample M, showing lamellar μ phase within the Nd-rich phase.

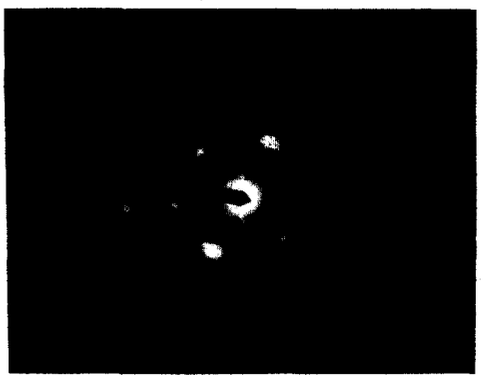

Fig. 6. Electron diffraction pattern (perpendicular to c axis) of the 2H variant of the μ phase within the Nd-rich phase (sample M).

that the preferential crystallization of the 2H-type variant is favoured either by higher growth kinetics or by a lower enthalpy of formation resulting from element addition.

EDX composition measurements reveal that Co is the only significant additive of the μ phase in relation to the ternary Nd–Fe–Al compound (about 5 at.% Co substituted to Fe; see Table 3). The approximately similar Co:Fe ratios in the μ phase and in the magnet implies that the μ-phase occurs, regardless of the transition metal, Fe or Co. No steric effect (the atomic radius of Fe is 0.126 nm against 0.125 nm for Co) or electronegativity effect (same values for Fe and Co) are expected from such a substitution. However, we may assume that the enhanced electron concentration per atom resulting from this Co substitution could play an important role in stabilizing the 2H variant. The effect of the electron concentration per atom on the stabilization of the different polytypic variants has already been demonstrated in other kinds of compound [13]. In these cases, it has been shown that the 2H-type variant was favoured by higher values of this concentration.

Table 3
Comparison of the phase μ in ternary Fe–Nd–Al alloys and in the magnet, giving composition and lattice parameters

	Fe–Nd–Al alloys (samples S1 and S2) [a]	Fe–Nd–B (–Al) (sample M) [b]
Typical composition (at.%)		
Nd	32	32
Dy	0	0
Fe	bal	57
Co	0	5
Al	2.5 to 5	6
Lattice parameters		
a (nm)	1.65	1.75
c_0 (nm)	1.20	1.47
$\gamma = 2c_0/a$	$1.46 = 2 \times 0.73$	$1.68 = 2 \times 0.84$

[a] Several sequences identified.
[b] 2H sequence.

The crystallographic parameters a and c_0 of the structural unit were derived from electron diffraction patterns. They are reported in Table 3 for both compounds observed in alloys S and M. We found that a very important expansion of the structural unit occurs in the three directions of the lattice, but particularly along the c axis. On extrapolating the crystallographic data from the ternary Fe–Nd–Al alloy, the calculated axial ratio for the simplest 2H sequence should be $\gamma = 2c_0/a = 1.46$. The actual value measured in sintered magnets is $\gamma = 1.68$. Therefore, the axial ratio of the 2H-type variant in the magnet adjusts to a value very close to that of the ideal hexagonal close packed arrangement ($\gamma = 1.63$).

Such an expansion of the 2H-type variant is not yet clearly understood. This effect seems to be too important to be attributed to a compositional dilatation. It more probably results from a structural modification of the compound. In this sense, the 2H-type variant should not be regarded as a true variant of the polytype μ phase, like the other stacking sequences already found, but instead as a definite thermodynamic phase, i.e. a polymorphic form of the μ phase. The existence of such anomalies in the stacking sequence of several polytypes has been known for a long time. For SiC, for instance, two variants – 2H and 3C (i.e. cubic β-SiC) – are known to exhibit a quite different behaviour from that of the numerous other α-SiC stacking sequences [5].

As shown in Fig. 5, the (001) lattice fringes (perpendicular to the c axis) highlight that the μ-phase crystals are deformed as a result of the mechanical strength that arises during solidification of the surrounding Nd-rich phase. This implies that the μ phase solidifies before (i.e. at a higher temperature than) the Nd-rich liquid phase.

The precipitates of the μ phase detected within the Nd-rich phase of sample M exhibit the same features as in samples S: lamellar morphology, facets and branching. The connection between the two parts of the branched crystal is not crystallographically perfect but is constituted of a perturbated lattice.

The lamella plane is normal to the c axis, clearly indicating that the crystal growth is easier perpendicular to this axis. This is attributed to a weak cohesion energy value between the largely spaced (001) planes. As a result, these planes cleave easily, which agrees with the observation of straicase-shaped crystals parallel to the basal plane. The crystals also exhibit a strong preferential thinning effect during sample preparation [14]. Such effects are not unusual for polytypic compounds.

In addition to its formation inside the triple junction Nd-rich phase, the μ phase has sometimes been detected at grain boundaries along the matrix Φ phase in the magnet. In such a case, the size of the μ-phase platelets was typically of the order of several nanometres. This indicates that the formation of the μ phase in the magnet is a two-step metallurgical process.

The formation of platelets of the ferromagnetic μ phase around Φ-phase grains is relevant information to understand the magnet coercivity enhancement resulting from Al addition. Since the μ phase exhibits a high uniaxial magnetocrystalline anisotropy at room temperature [2], this compound could act as a pinning phase for the domain wall of the matrix Φ phase. This would require that the corresponding domain wall energy in the μ phase (unknown value) were lower than that in the Φ phase (about 30 mJ m^{-2}) [15]. Such an assumption has to be experimentally confirmed.

4. Conclusions

The μ phase has been identified in an Al-substituted Nd–Fe–B magnet. A microstructural comparison with Nd–Fe–Al ternary alloys shows striking similarities between the morphology of the μ phase in the sintered magnet and in the ternary alloys. This suggests that the solidification mechanism of the μ phase is the same in both materials, replacing the Φ phase in the sintered magnet by Nd_2Fe_{17} in the ternary alloys.

First, thin platelets of the μ phase solidify along Φ-phase grains (Nd_2Fe_{17} grains respectively) by a peritectic reaction between this compound and the melt.

Secondly, branched eutectic lamellae of the μ phase form inside the Nd-rich phase, from the remaining Nd-rich liquid.

However, several crystallographic differences are noticed in both alloys (modified lattice parameters, different stacking variants), suggesting the existence of a structural modification of the μ phase. This assumption is in agreement with the recent identification of a compound closely related to the μ phase in a binary Nd–Fe alloy [16].

Acknowledgments

We acknowledge AIMANTS UGIMAG SA (Saint-Pierre d'Allevard, France) for providing the UGISTAB 215-XH magnet (sample M), and B. Grieb from Max-Planck Institute (Stuttgart, Germany) for providing the Nd–Fe–Al alloy (sample S1).

References

[1] K.G. Knoch, *Thesis*, University of Stuttgart, 1990.
[2] B. Grieb, *Thesis*, University of Stuttgart, 1991.
[3] P. Magnin and W. Kurz, Solidification des alliages, in F. Durand (ed.), *Ecole d'été Carry-le-Rouët, 9–14 September 1985*, Les Éditions de Physique, Paris, 1988, pp. 169–190.
[4] J. Delamare, D. Lemarchand and P. Vigier, *J. Magn. Magn. Mater., 104–107* (1992) 1092–1093.
[5] A.R. Verma and P. Krishna, *Polymorphism and Polytypism in Crystals*, Wiley, New York, 1966.
[6] J. Delamare et al., to be published.
[7] J. Bernardi, J. Fidler and F. Födermayr, *INTERMAG 92 Conf., Saint Louis, MO, 13–16 April 1992.*
[8] J. Bras, K. Biyadi, M. Fagot, J. Degauque, F. Vial and P. Tenaud, *J. Magn. Magn. Mater., 101* (1991) 369–371.
[9] P. Tenaud, F. Vial and M. Sagawa, *IEEE Trans. Magn., 26* (1990) 1930–1932.
[10] M. Sagawa, P. Tenaud, F. Vial and K. Hiraga, *IEEE Trans. Magn., 26* (1990) 1957–1959.
[11] D. Lemarchand, B. Labulle and P. Vigier, *J. Phys. Coll. C8, Suppl. 12, 49* (1988) 637.
[12] K.G. Knoch, T.-Th. Henig and J. Fidler, *J. Magn. Magn. Mater., 83* (1990) 209.
[13] Y. Komura, *Phase Transit., 16–17* (1989) 495–507.
[14] J. Delamare, *Thesis*, University of Rouen, 1992.
[15] K.H.J. Buschow, *Mater. Sci. Rep., 1* (1986) 1–64.
[16] J. Delamare, D. Lemarchand, P. Vigier, F.P. Missel and F.J.G. Landgraf, *Proc. ICEM 13, Paris 17–22 July 1994, Les Éditions de Physique, 2B* (1994) 1181.